Published in final edited form as:
Int J Cancer. 2014 September 1; 135(5): 1238–1246. doi:10.1002/ijc.28747.

Oncolytic Vaccinia Virus Demonstrates Anti-angiogenic Effects Mediated by Targeting of VEGF

Weizhou Hou[2], **Hannah Chen**[2], **Juan Rojas**, **Padma Sampath**, and **Steve H Thorne**[1]
Department of Surgery, University of Pittsburgh Cancer Institute, University of Pittsburgh, PA USA

Abstract

Oncolytic vaccinia virus has been shown to induce a profound, rapid and tumor-specific vascular collapse in both preclinical models and in clinical studies, however a complete examination of the kinetics and levels of collapse and revascularization has not been described previously. Contrast-enhanced ultrasound was used to follow tumor perfusion levels in mouse tumor models at times after vaccinia therapy. It was observed that re-vascularization after viral therapy was dramatically delayed and did not occur until after viral clearance. This indicated that oncolytic vaccinia may posses a previously undescribed anti-angiogenic potential that might synergize with the reported anti-vascular effects. Despite a rapid loss of perfusion and widespread hypoxia within the tumor it was observed that VEGF levels in the tumor were suppressed throughout the period of active viral infection. Although tumor vasculature could eventually reform after the viral therapy was cleared in mouse models, anti-tumor effects could be significantly enhanced through additional combination with anti-VEGF therapies. This was initially examined using a gene therapy approach (Ad-Flk1-Fc) to target VEGF directly, demonstrating that the timing of application of the anti-angiogenic therapy was critical. However, it is also known that oncolytic vaccinia sensitizes tumors to tyrosine kinase inhibitors (TKI) in the clinic through an unknown mechanism. It is possible this phenomenon may be mediated through the anti-angiogenic effects of the TKIs. This was modeled in mouse tumors using sunitinib in combination with oncolytic vaccinia. It was observed that prevention of angiogenesis mediated by oncolytic vaccinia can be utilized to enhance the TKI therapy.

Keywords

Oncolytic virus; anti-vascular; anti-angiogenic; VEGF; Tyrosine Kinase Inhibitor

INTRODUCTION

Oncolytic viruses are cancer therapies based on viral strains that selectively replicate in tumor cells, either naturally or through genetic modification[1, 2]. This platform has received significant attention recently as results form encouraging Phase II and III trials have been

[1]Corresponding Author; 1.46e Hillman Cancer Center, 5117 Centre Avenue, Pittsburgh, PA 15238, USA ThorneSH@UPMC.edu Fax No. 412 623 7709 Tel No 412 623 4896.
[2]Contributed equally to this work

Conflict of Interest: SHT has a financial interest in Jennerex Inc.

reported and several different vectors are undergoing randomized clinical testing[3-6]. One of these vectors is based on a vaccinia virus backbone[7], while several further vaccinia-based oncolytic vectors have successfully entered earlier stage clinical testing[8, 9].

One reason for the success of oncolytic virotherapy is the capacity of the agents to target the tumor through multiple mechanisms independent from those typically utilized by more traditional chemotherapies and radiotherapy[2]. This includes direct tumor cell destruction resulting from viral replication as well as the overcoming of localized immune suppression within the tumor and induction of a systemic anti-tumor immune response. More recently a further mechanism has been described for several viruses, including vaccinia, both in pre-clinical models and in clinical studies[10-13]. This involves the targeting of tumor-associated endothelial cells leading to a rapid destruction of the tumor vasculature and loss of perfusion within the tumor. However, this process is poorly understood and despite apparent profound and rapid loss of tumor perfusion, complete responses remain elusive and tumor regrowth typically still occurs implying that revascularization and neo-angiogenesis must eventually occur.

It was therefore decided to model the process of neo-angiogenesis within the tumor subsequent to viral induced vascular collapse. A detailed quantification of the reduction in tumor perfusion levels and the kinetics of re-vascularization during and after clearance of the viral therapy in mouse tumor models would help define how best to combine oncolytic vaccinia with other therapeutics. Unexpectedly tumor perfusion remained suppressed during the entire period of viral infection, implying that oncolytic vaccinia therapy produces previously unreported antiangiogenic effects. It was determined that the level of VEGF within the tumor was also significantly reduced during this period, despite the induction of hypoxic conditions within the tumor, and that this suppression of VEGF was sustained throughout the period of active viral replication within the tumor. VEGF concentrations in the tumor then returned to baseline levels soon after viral clearance and prior to tumor re-vascularization.

Approaches that prevent regrowth of treated tumors through additional prevention of revascularization after viral clearance are therefore attractive, however detailed attempts to enhance or capitalize on vascular collapse through logical combination of oncolytic viruses with anti-angiogenic therapies have not been reported to date. Application of therapeutics that target VEGF and angiogenesis would be expected to be most effective if applied at the interface between viral clearance and re-vascularization. This was initially examined by combining oncolytic vaccinia with an anti-angiogenic gene therapy approach (Ad-Flk1-Fc). In addition, oncolytic vaccinia virotherapy has demonstrated the capacity to sensitize even previously resistant tumors to some tyrosine kinase inhibitors in the clinic, and vaccinia-TKI combination therapy is being explored in randomized testing. Because many TKI possess antiangiogenic properties, the targeting of the vasculature may represent the reason for this synergistic activity. This possibility was also explored in mouse tumor models.

MATERIALS AND METHODS

Cell Lines and Viruses

Cell lines MDA-MB-231 (human breast cancer), 4T1 (mouse breast cancer) and RENCA (mouse renal cell cancer) were obtained form ATCC and grown in recommended media. HUVEC cells were obtained from Lonza (Allendale, NJ).

Virus strain vvDD-luc has been described previously[14]. Viral strain vvDD-Flk1-Fc was constructed for this work and additionally contained Flk1-Fc expressed from the p7.5 promoter from within the thymidine kinase locus.

The non-replicating Adenovirus strain Ad-Flk1-Fc has also been described previously[15].

Cell Culture Assays

ELISA for VEGF (R&D Systems, Minneapolis, MN) was run on conditioned media collected after 24h.

Proliferation assay on HUVEC cells were run with a BrdU proliferation kit (Roche, Indianapolis, IN). BrdU was added in fresh medium or medium as indicated for 48h, BrdU was then stained according to manufacturer's instructions and BrdU positive cells (4x fields with >200 cells) counted under an inverted microscope. Recombinant $VEGF_{165}$ (R&D systems) was added at 25ng/ml.

Mouse Tumor Models

Female BALB/c and athymic nu-/nu- mice were obtained from Jackson at 8 weeks old and tumors were implanted through subcutaneous injection of 1×10^6 mouse tumor cells or 2×10^7 human tumor cells. Treatments were begun when tumors reached 50-100mm^3 (unless otherwise stated) and subsequent tumor growth was followed by caliper measurement. Mice were sacrificed (and considered 'dead' for survival studies) when tumors reached 1400mm^3. Treatments included intravenous (tail vein) injection of 1×10^8 PFU of vaccinia virus or 1×10^{10} PFU of Ad Flk1-Fc. Sunitinib was given at 40mg/kg for 7 consecutive days through intraperitoneal injection. In some experiments a single IP injection of 50mg/kg combretastatin A4 Phosphate was given.

All animal studies were run according to protocols approved by the University of Pittsburgh Institute on Animal Care and Use Committee.

Small Animal Imaging Studies

Contrast-enhanced ultrasound imaging of vasculature and perfusion was performed on the tumor and the surrounding tissue. Mice were anesthetized (2% isoflurane) and their tail vein cannulated. Ultrasound imaging was performed using a Vevo770 small animal ultrasound system with an RMV704 scanhead (VisualSonics) before and during intravenous injection of 100ul of Vevo MicroMarker Non-Targeted Contrast Agent (VisualSonics). Tumor perfusion was determined as rate of grayscale intensity change (accumulation of contrast agent in the region of interest) per second over the first 5 seconds after systemic delivery of non-targeted contrast agent. Perfusion rates were determined for different regions of interest

(tumor and non-tumor) and calculated using the Vevo software (VisualSonics). (n=3 per group, experiment repeated three times).

Bioluminescence imaging was also performed to quantify viral luciferase transgene expression levels. Mice were injected with luciferin substrate (30mg/kg IP; GoldBio) prior to imaging on an IVIS200 system (Perkin Elmer). Bioluminescence signal was quantified using the LivingImage software (Perkin Elmer).

Immunohistochemistry

Tumors were also recovered post mortem at pre-determined times from mice treated in different ways and fixed in 2% paraformaldehyde before being flash frozen. Tumor sections were stained either with rat anti-mouse CD31 (BD Pharmingen) or with annexin V, as well as polyclonal anti-vaccinia FITC conjugated antibody (abcam). At least 5 sections were analyzed from each tumor and multiple (at least 10) fields of view examined by fluorescence microscopy for each section.

In addition tumor hypoxia was determined using Hypoxyprobe (Hypoxyprobe, Inc.) according to manufacturer's guidelines, with Hypoxyprobe injected intravenously 15 minutes prior to animal sacrifice and counterstained in sections post mortem. Sections were photographed blinded at 200X magnification.

Statistics

Student's T-test used for all statistical analyses, except for survival curves, where Mantel-Cox log-rank tests were used. Significance was considered at $p<0.05$.

RESULTS

Oncolytic vaccinia virotherapy results in rapid loss of perfusion, with reperfusion occurring only after clearance of the viral vector

In order to better understand the effects of oncolytic vaccinia viral therapy on tumor vasculature and perfusion and how this might be enhanced through combination therapy, it was necessary to more clearly define the kinetics, levels and mechanisms behind the vascular collapse and presumed revascularization during tumor relapse.

In initial studies, contrast-enhanced ultrasound was used to examine both rates of perfusion and the overall levels of vascularity of syngeneic tumors implanted subcutaneously into mice at times before and after treatment with oncolytic vaccinia (Fig 1). BALB/c mice were implanted with 4T1 tumors and viral therapy was via tail vein injection of 1×10^8 PFU of vvDD-luc (vaccinia virus double deleted[8, 14]; vaccinia strain WR with deletions in the viral growth factor (VGF) and thymidine kinase (TK) genes and expressing luciferase). It was observed that, as expected from our previous results with the similar WR.TK- virus[10], perfusion within the tumor dropped dramatically (over 50-fold) to almost undetectable levels within 48h of intravenous delivery of virus (Fig 1). However, previous studies had not determined the kinetics, level or properties of any subsequent revascularization. Here we observed that revascularization had begun by 10 days after initial treatment. The fact complete revascularization had not occurred by this time was somewhat surprising as many

reports with classic anti-vascular agents such as combrestatin A4 phosphate (CA4P) demonstrate that re-vascularization is rapid, typically being completed within 72h of initial therapy induced vascular collapse [16].

A more detailed analysis of the kinetics and levels of vascular collapse and recovery were therefore performed (Fig 2A). In addition, viral replication, biodistribution and persistence were determined by bioluminescence imaging of luciferase transgene expression from the viral vector (Fig 2B) and tumor burden was followed with caliper measurement (Fig 2C).

It was observed that the perfusion in the tumor remained suppressed for at least 7 days, and only began to re-vascularize from around 10 days after initial treatment (Fig 2A). The timing of this revascularization was potentially significant as it coincided closely with the timing of clearance of virus from the tumor (Fig 2B), implying that viral presence within the tumor may be sufficient to inhibit angiogenesis. It was also notable that tumor growth subsequent to treatment appeared to occur in several distinct phases (Fig 2C), with tumor growth effectively blocked for the first 7-10 days after viral treatment (while active viral replication continues within the tumor), followed by a period of slow tumor re-growth (10 to 20 days after treatment), during which time re-vascularization was occurring, and a period of rapid tumor growth beginning around 20 days after initial treatment that coincided with the effective completion of tumor re-vascularization.

Oncolytic Vaccinia virotherapy antiangiogenic properties are apparently mediated by targeting of VEGF *in vivo*

The observation that oncolytic vaccinia virotherapy treatment both induces rapid vascular collapse and subsequently prevents revascularization (Fig 1&2) implies that the viral therapy has some form of antiangiogenic capacity. In order to determine if this sustained prevention of tumor reperfusion after vaccinia therapy is due to ongoing viral-mediated targeting of tumor vasculature, or if vaccinia possesses additional and novel anti-angiogenic properties we examined the effects in the tumor microenvironment.

As expected, the reduction in tumor perfusion resulted in widespread hypoxia within the treated tumor (Fig 3A). This also correlated with increased apoptosis throughout the tumor, even in regions uninfected with virus (Fig 3B). However, of particular interest was the observation that VEGF levels within the tumor were significantly reduced after viral treatment and remained suppressed during the period of viral infection (Fig 3C). This is surprising as the induction of hypoxic conditions would normally be expected to lead to increases in local VEGF levels and indicates that oncolytic vaccinia therapy indeed has an additional and previously unreported anti-angiogenic mechanism of action. This observed drop in VEGF levels was maintained during the period of viral infection of the tumor and returned to baseline levels soon after viral clearance and prior to revascularization (Fig 3C). The suppression of VEGF would explain why the revascularization and re-perfusion of the tumor did not effectively commence until after the virus had been cleared. Because tumor volume remains constant in this model (Fig 2C), reduction in VEGF levels cannot be simply due to reduction in tumor burden.

Oncolytic Vaccinia viral infection reduces tumor VEGF production *in vitro* and limits endothelial cell proliferation

In order to examine the direct effects of viral infection on VEGF production from tumor cells, ELISA's were run on media collected from 4T1 and RENCA cells after infection with vaccinia at different multiplicities of infection (MOIs). It was found that vaccinia reduced VEGF production even when used at very low MOIs, indicating not only a direct reduction in VEGF production from infected cells (at times prior to cell lysis), but that a bystander effect occurred, with infected cells secreting some factor that reduces VEGF production by surrounding uninfected cells. For example, RENCA cells infected at an MOI of 0.1 (meaning that less than 10% of cells are infected) resulted in reduction of VEGF production of over 98% (Fig 4A). It is unclear how the virus is acting to suppress VEGF levels or what contribution the depletion of endothelial cells in the tumor may play *in vivo* in reducing VEGF levels (this is currently under investigation).

In follow up studies, spent media from the same treatments in 4T1 cells were filter sterilized (to remove any viral particles) and used to stimulate proliferation in HUVEC cells as determined by BrDU incorporation (Fig 4B). It was seen that whereas media from uninfected 4T1 cells could stimulate proliferation, infection of the 4T1 cells with oncolytic vaccinia meant the conditioned media could no longer stimulate proliferation. This effect was overcome by the addition of recombinant VEGF to the media, indicating that a block of VEGF production or activity was indeed mediating the anti-angiogenic effects of vaccinia virus.

Combining Oncolytic Vaccinia and Anti-Angiogenic Gene Therapy Results in Further Enhanced Therapeutic Benefit but Timing is Critical

Because elevation of VEGF levels and re-vascularization commences after viral clearance it is possible that application of anti-angiogenic therapies at this time could significantly enhance therapeutic benefit. The benefits of applying anti-angiogenic therapies after anti-vascular therapies have been demonstrated in the clinic[17], and this effect may be increased further in combination with oncolytic vaccinia due to vaccinia's both vascular disrupting and anti-angiogenic properties. In order to examine this hypothesis, oncolytic vaccinia was combined with an anti-angiogenic gene therapy approach. The Flk1-Fc gene consists of a soluble, VEGF binding ectodomain from Flk1 (VEGF-R2/ KDR), conjugated to the murine IgG2α Fc domain to enhance protein stability in circulation [15]. This gene product acts as a VEGF competitive binding protein, and has been shown to combine with oncolytic adenovirus[18], as well as to enhance the anti-tumor effects of oncolytic vaccinia[19]. However, in these previous studies Flk1-Fc was expressed concurrently with oncolytic viral activity, whereas our data has determined that increases in VEGF levels and re-vascularization occur primarily after the oncolytic vector has been cleared.

We therefore looked to initially determine the effects of combining oncolytic vaccinia with a purely anti-angiogenic therapy in order to examine the importance of timing of addition of the two therapies. In order to dissociate the anti-angiogenic effects of Flk1-Fc from any additional effects due to its expression form an oncolytic virus we expressed the Flk1-Fc from a non-replicating Adenovirus. In this way, the non-replicating Adenovirus expressing

Flk1-Fc could be applied at different times during or after application of oncolytic vaccinia to tumor bearing mouse models (Fig 5A). Because the Ad Flk1-Fc vector is most effective against human tumors, a human breast cancer cell line (MDA-MB-231) was used in an immunodeficient mouse model for this study. The Adenovirus backbone is non-replicating due to an E1A deletion, and so is purely a gene expression system with no direct oncolytic or therapeutic effect, as has been shown previously. It was observed that expression of Flk1-fc at time points after viral clearance (beginning 7 days after initial vvDD therapy) resulted in 80% complete responses and provided dramatic and significant therapeutic advantage relative to the same combination with the two therapies applied concurrently (Fig 5A). In further experiments an oncolytic vaccinia strain expressing Flk1-Fc as a transgene was also incorporated, it was again confirmed that applying the anti-angiogenic vector after vvDD clearance provided significant therapeutic advantage (Fig 5B), again demonstrating that blocking re-vascularization after clearance of the virus resulted in the optimal therapeutic benefit. This is despite the fact that vvDD-Flk1-Fc secretes higher levels of Flk1-Fc than the Adenovirus system, and produces the transgene exclusively from within the tumor (whereas the Adenovirus system expresses primarily from the liver).

Sunitinib (Sutent) Combination with Oncolytic Vaccinia Results in Significantly Enhanced Anti-tumor Effects

Oncolytic vaccinia virus has displayed promising results in clinical testing, particularly in combination with tyrosine kinase inhibitors, with some data indicating that viral treatment can even sensitize previously resistant tumors to VEGF-R targeting tyrosine kinase inhibitors [5]. However the mechanisms behind the clinical success of this combination are so far undefined. Of special note, one recent report describes an exciting clinical response in an RCC patient treated with a combination of oncolytic vaccinia followed by sunitinib making combination with this TKI of special interest[20]. In addition, because the Ad-Flk1-Fc vector has not been tested clinically, combining this with oncolytic vaccinia in a clinical setting would be technically complex.

It was therefore decided to examine the combination of oncolytic vaccinia with sunitinib (Sutent), a tyrosine kinase inhibitor that blocks both VEGF and PDGF signaling (as well as acting on several other tyrosine kinases including KIT) and an FDA approved agent for treatment of RCC and GIST [21, 22]. In this way it may be possible to examine the role of vascular targeting in the reported clinical success of this combination. Previous reports have extensively studied the effects of sunitinib on both 4T1 and RENCA tumors [23], and found that at the doses used *in vivo* this drug has no effect on either 4T1 or RENCA cell proliferation or survival. It was also seen that the TKI had no effect on immune cell infiltrate in the tumors (especially on the levels of myeloid cells). This means that the *in vivo* effects are likely to be primarily mediated through the action of sunitinib on endothelial cells (although effects on other targets of the tyrosine kinase inhibitor cannot be ruled out).

It is also of note that many tyrosine kinase inhibitors (including sunitinib) block vaccinia release from infected cells[24], so limiting viral spread and acting as anti-viral agents, meaning that concurrent addition of both therapies would be expected to be antagonistic.

However, because sunitinib will be added before or after viral infection in these studies this is not considered to be an issue.

Initial studies examined combinations of vvDD and sunitinib (with sunitinib added 7 days after vvDD treatment) in the 4T1 model, and determined that the combination led to significantly increased anti-tumor effects (Fig 6A). These benefits were even seen when large primary tumors were treated (right panel) and are especially dramatic as sunitinib alone had no effect on overall tumor growth. This indicates that the combination has synergsistic effects (as sunitinib significantly enhanced vvDD therapy, but had no effect when used alone) with vvDD therapy apparently 'sensitizing' the tumor to subsequent sunitinib treatment.

Because sunitinib is approved for the treatment of RCC, a second mouse tumor model was also incorporated alongside the previously examined 4T1 (breast cancer) model, incorporating renal cancer (Renca) cells implanted subcutaneously into BALB/c mice. Initial studies of tumor perfusion determined that the anti-vascular effects of vvDD treatment in the Renca model were not as dramatic as that for 4T1 (Fig 6B), primarily because the Renca tumors have a reduced level of baseline perfusion relative to the 4T1 tumor model (as has been previously reported [23]). In this model sunitinib alone does have a small therapeutic effect (apparently as the RENCA cells are less capable of responding to increased hypoxia by inducing glycolysis, as was reported with the 4T1 model [23]). However, despite this, the combination of vvDD followed by sunitinib again significantly increased the overall survival benefit (Fig 6C). Of further interest, in this model the same combination was also tried in the opposite order (sunitinib followed by vvDD 7 days later) and, as with Flk1-Fc, it was seen that the additional therapeutic benefits were only seen when the oncolytic vaccinia vector was added first.

DISCUSSION

The recent confirmation of vaccinia-induced tumor vascular collapse in a clinical setting [13] means that a more thorough understanding of the kinetics and levels of vascular collapse and subsequent recovery are warranted. This was undertaken using contrast enhanced ultrasound in tumor-bearing mice, such that perfusion rates can be followed systematically in real time in a single living animal.

This initially confirmed previous studies by us and other groups indicating vaccinia-induced vascular collapse within the tumor is both rapid and extensive. Although one other recent report found that oncolytic vaccinia virus alone was not capable of inducing vascular collapse, this may have been related to the model being used (with canine tumors implanted into immunodeficient mice)[25].

Because single viral therapy is rarely curative in the 4T1 model we used it was assumed re-vascularization must occur during tumor relapse. It was also predicted that re-vascularization would likely occur with similar kinetics to that seen with classic vascular disrupting agents [16]. Instead it was seen that tumor perfusion remained suppressed throughout the entire period of ongoing viral infection within the tumor. Indeed reduced

perfusion rates appeared to more closely correlate with delay in tumor growth than ongoing viral infection. It was predicted that this unexpected observation might be either due to an ongoing anti-vascular effect or due to a novel anti-angiogenic mechanism of tumor suppression mediated by the viral therapy.

The observation that levels of VEGF, a classic mediator of angiogenesis, were also suppressed within the tumor during the period of viral infection implied that an anti-angiogenic mechanism was at least partially contributing to the prevention of revascularization. VEGF levels were reduced despite the production of extensive hypoxic conditions within the tumor, leading to widespread apoptosis, and reductions in VEGF production were also demonstrated in cell culture assays. Together this data indicates that vaccinia possesses a potent anti-angiogenic potential that compliments its anti-vascular effects during tumor therapy. This capability might confer an advantage on poxviruses during the course of natural infections, where the formation of dermal pustules might benefit from an inhibition of angiogenesis. The exact molecular mechanisms mediating this targeting of VEGF are currently under investigation, but it is of interest that the effects appear to be conferred on uninfected cells within a population infected at a low MOI (i.e. infection rates of less than 10% of cells still resulted in >95% reduction in VEGF release). It is not currently known how the virus suppresses VEGF production, or if any secreted factor is viral or host cell derived. However, ongoing studies are beginning to define the mechanism.

This observation does open up new possibilities for combination therapies, where the addition of anti-angiogenic agents might provide significant therapeutic benefit if added directly after clearance of the viral therapy. This was initially tested using a primarily research based anti-angiogenic gene therapy approach (primarily in order to confirm any therapeutic benefits are mediated through vascular targeting). It was confirmed that anti-angiogenic therapies provide dramatic therapeutic benefit if added at times immediately after viral clearance. Together this data supports the hypothesis that direct viral effects on vasculature and VEGF levels are capable of suppressing angiogenesis during the period of viral infection, and that further combination with additional anti-angiogenic therapies can be highly effective, especially when these are added at times after viral clearance. This result explains why the expression of anti-angiogenic genes from oncolytic viruses has previously resulted in only small therapeutic benefit [19, 25, 26].

It is perhaps significant that many of the most dramatic responses reported in the clinic during testing of oncolytic vaccinia have been during combination with tyrosine kinase inhibitors [20, 27], many of which directly target mediators of angiogenesis such as the VEGF and PDGF pathways, especially with the TKI added after viral treatment. The reasons behind the therapeutic benefits of these combinations was not previously understood, however data produced here would indicate blocking of angiogenesis and prevention of revascularization may be a key factor. This was modeled in several different mouse tumors, with combinations of oncolytic vaccinia and the TKI sunitinib producing additional therapeutic benefits *in vivo*, but only if the viral therapy was added first. This is despite the sunitinib being used at doses that have no direct effect on the tumor cells *in vitro* and occurs even if the sunitinib alone has no effect on tumor growth *in vivo* (with viral therapy

apparently ‘sensitizing’ the tumor to subsequent TKI therapy). Although model systems were incorporated where sunitinib had no measurable direct effects on the tumor cells or on the level and type of tumor immune infiltrate, the fact that both TKI and oncolytic vaccinia target multiple phenotypic properties of cancers means that other factors beyond endothelial cell targeting may also contribute to the benefits of these combinations.

Overall however, it is felt that the promising nature of these combinations means that further clinical testing of oncolytic vaccinia and anti-angiogenic therapies is warranted.

Acknowledgments

This work was supported directly by NIH grant R01 CA140215. In addition core facilities used in this work were supported by P30 CA047904-21S3. We thank Melissa Bigger for help with some imaging studies.

REFERENCES

1. Guo ZS, Thorne SH, Bartlett DL. Oncolytic virotherapy: Molecular targets in tumor-selective replication and carrier cell-mediated delivery of oncolytic viruses. Biochim Biophys Acta. 2008
2. Kirn DH, Thorne SH. Targeted and armed oncolytic poxviruses: a novel multi-mechanistic therapeutic class for cancer. Nat Rev Cancer. 2009; 9:64–71. [PubMed: 19104515]
3. Schmidt C. Amgen spikes interest in live virus vaccines for hard-to-treat cancers. Nature biotechnology. 2011; 29:295–6.
4. Breitbach CJ, Burke J, Jonker D, Stephenson J, Haas AR, Chow LQ, Nieva J, Hwang TH, Moon A, Patt R, Pelusio A, Le Boeuf F, et al. Intravenous delivery of a multi-mechanistic cancer-targeted oncolytic poxvirus in humans. Nature. 2011; 477:99–102. [PubMed: 21886163]
5. Park BH, Hwang T, Liu TC, Sze DY, Kim JS, Kwon HC, Oh SY, Han SY, Yoon JH, Hong SH, Moon A, Speth K, et al. Use of a targeted oncolytic poxvirus, JX-594, in patients with refractory primary or metastatic liver cancer: a phase I trial. Lancet Oncol. 2008; 9:533–42. [PubMed: 18495536]
6. Heo J, Reid T, Ruo L, Breitbach CJ, Rose S, Bloomston M, Cho M, Lim HY, Chung HC, Kim CW, Burke J, Lencioni R, et al. Randomized dose-finding clinical trial of oncolytic immunotherapeutic vaccinia JX-594 in liver cancer. Nature Medicine. 2013; 19:329–36.
7. Kim JH, Oh JY, Park BH, Lee DE, Kim JS, Park HE, Roh MS, Je JE, Yoon JH, Thorne SH, Kirn D, Hwang TH. Systemic Armed Oncolytic and Immunologic Therapy for Cancer with JX-594, a Targeted Poxvirus Expressing GM-CSF. Mol Ther. 2006; 14:361–70. [PubMed: 16905462]
8. Thorne SH, Hwang TH, O'Gorman WE, Bartlett DL, Sei S, Kanji F, Brown C, Werier J, Cho JH, Lee DE, Wang Y, Bell J, et al. Rational strain selection and engineering creates a broad-spectrum, systemically effective oncolytic poxvirus, JX-963. J Clin Invest. 2007; 117:3350–8. [PubMed: 17965776]
9. Zhang Q, Yu YA, Wang E, Chen N, Danner RL, Munson PJ, Marincola FM, Szalay AA. Eradication of solid human breast tumors in nude mice with an intravenously injected light-emitting oncolytic vaccinia virus. Cancer Res. 2007; 67:10038–46. [PubMed: 17942938]
10. Kirn DH, Wang Y, Le Boeuf F, Bell J, Thorne SH. Targeting of interferon-beta to produce a specific, multi-mechanistic oncolytic vaccinia virus. PLoS Med. 2007; 4:e353. [PubMed: 18162040]
11. Breitbach CJ, Paterson JM, Lemay CG, Falls TJ, McGuire A, Parato KA, Stojdl DF, Daneshmand M, Speth K, Kirn D, McCart JA, Atkins H, et al. Targeted inflammation during oncolytic virus therapy severely compromises tumor blood flow. Mol Ther. 2007; 15:1686–93. [PubMed: 17579581]
12. Liu TC, Hwang T, Park BH, Bell J, Kirn DH. The targeted oncolytic poxvirus JX-594 demonstrates antitumoral, antivascular, and anti-HBV activities in patients with hepatocellular carcinoma. Mol Ther. 2008; 16:1637–42. [PubMed: 18628758]

13. Breitbach CJ, Arulanandam R, De Silva N, Thorne SH, Patt R, Daneshmand M, Moon A, Ilkow C, Burke J, Hwang TH, Heo J, Cho M, et al. Oncolytic vaccinia virus disrupts tumor-associated vasculature in humans. Cancer Research. 2013; 73:1265–75. [PubMed: 23393196]
14. McCart JA, Ward JM, Lee J, Hu Y, Alexander HR, Libutti SK, Moss B, Bartlett DL. Systemic cancer therapy with a tumor-selective vaccinia virus mutant lacking thymidine kinase and vaccinia growth factor genes. Cancer Res. 2001; 61:8751–7. [PubMed: 11751395]
15. Kuo CJ, Farnebo F, Yu EY, Christofferson R, Swearingen RA, Carter R, von Recum HA, Yuan J, Kamihara J, Flynn E, D'Amato R, Folkman J, et al. Comparative evaluation of the antitumor activity of antiangiogenic proteins delivered by gene transfer. Proc Natl Acad Sci U S A. 2001; 98:4605–10. [PubMed: 11274374]
16. Li J, Chen F, Feng Y, Cona MM, Yu J, Verbruggen A, Zhang J, Oyen R, Ni Y. Diverse responses to vascular disrupting agent combretastatin a4 phosphate: a comparative study in rats with hepatic and subcutaneous tumor allografts using MRI biomarkers, microangiography, and histopathology. Transl Oncol. 2013; 6:42–50. [PubMed: 23418616]
17. Nathan P, Zweifel M, Padhani AR, Koh DM, Ng M, Collins DJ, Harris A, Carden C, Smythe J, Fisher N, Taylor NJ, Stirling JJ, et al. Phase I trial of combretastatin A4 phosphate (CA4P) in combination with bevacizumab in patients with advanced cancer. Clinical cancer research : an official journal of the American Association for Cancer Research. 2012; 18:3428–39. [PubMed: 22645052]
18. Thorne SH, Tam BY, Kirn DH, Contag CH, Kuo CJ. Selective intratumoral amplification of an antiangiogenic vector by an oncolytic virus produces enhanced antivascular and anti-tumor efficacy. Mol Ther. 2006; 13:938–46. [PubMed: 16469543]
19. Guse K, Sloniecka M, Diaconu I, Ottolino-Perry K, Tang N, Ng C, Le Boeuf F, Bell JC, McCart JA, Ristimaki A, Pesonen S, Cerullo V, et al. Antiangiogenic arming of an oncolytic vaccinia virus enhances antitumor efficacy in renal cell cancer models. Journal of virology. 2010; 84:856–66. [PubMed: 19906926]
20. Heo J, Breitbach CJ, Moon A, Kim CW, Patt R, Kim MK, Lee YK, Oh SY, Woo HY, Parato K, Rintoul J, Falls T, et al. Sequential Therapy With JX-594, A Targeted Oncolytic Poxvirus, Followed by Sorafenib in Hepatocellular Carcinoma: Preclinical and Clinical Demonstration of Combination Efficacy. Molecular therapy : the journal of the American Society of Gene Therapy. 2011
21. Demetri GD, van Oosterom AT, Garrett CR, Blackstein ME, Shah MH, Verweij J, McArthur G, Judson IR, Heinrich MC, Morgan JA, Desai J, Fletcher CD, et al. Efficacy and safety of sunitinib in patients with advanced gastrointestinal stromal tumour after failure of imatinib: a randomised controlled trial. Lancet. 2006; 368:1329–38. [PubMed: 17046465]
22. Motzer RJ, Hutson TE, Tomczak P, Michaelson MD, Bukowski RM, Rixe O, Oudard S, Negrier S, Szczylik C, Kim ST, Chen I, Bycott PW, et al. Sunitinib versus interferon alfa in metastatic renal-cell carcinoma. The New England journal of medicine. 2007; 356:115–24. [PubMed: 17215529]
23. Welti JC, Powles T, Foo S, Gourlaouen M, Preece N, Foster J, Frentzas S, Bird D, Sharpe K, van Weverwijk A, Robertson D, Soffe J, et al. Contrasting effects of sunitinib within in vivo models of metastasis. Angiogenesis. 2012; 15:623–41. [PubMed: 22843200]
24. Reeves PM, Bommarius B, Lebeis S, McNulty S, Christensen J, Swimm A, Chahroudi A, Chavan R, Feinberg MB, Veach D, Bornmann W, Sherman M, et al. Disabling poxvirus pathogenesis by inhibition of Abl-family tyrosine kinases. Nat Med. 2005; 11:731–9. [PubMed: 15980865]
25. Patil SS, Gentschev I, Adelfinger M, Donat U, Hess M, Weibel S, Nolte I, Frentzen A, Szalay AA. Virotherapy of canine tumors with oncolytic vaccinia virus GLV-1h109 expressing an anti-VEGF single-chain antibody. PLoS One. 2012; 7:e47472. [PubMed: 23091626]
26. Frentzen A, Yu YA, Chen N, Zhang Q, Weibel S, Raab V, Szalay AA. Anti-VEGF single-chain antibody GLAF-1 encoded by oncolytic vaccinia virus significantly enhances antitumor therapy. Proceedings of the National Academy of Sciences of the United States of America. 2009; 106:12915–20. [PubMed: 19617539]
27. Breitbach CJ, Thorne SH, Bell JC, Kirn DH. Targeted and armed oncolytic poxviruses for cancer: the lead example of JX-594. Curr Pharm Biotechnol. 2012; 13:1768–72. [PubMed: 21740365]

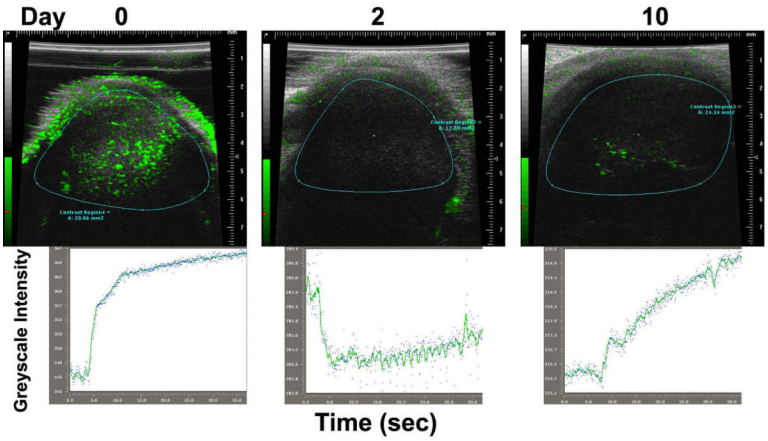

Figure 1.

Oncolytic vaccinia virus induces a reversible vascular collapse in the tumor as determined by contrast enhanced ultrasound. Contrast enhanced ultrasound was used to determine vascularity and perfusion rates in vvDD treated tumors. Mice (BALB/c) with subcutaneous 4T1 tumors implanted on the hind limb were treated intravenously with 1×10^8 PFU of vvDD-Luc when tumors became palpable (50-100mm^3, day 0). Images of tumor vasculature were created through intravenous injection of non-targeted contrast enhanced microbubbles at different times (top), while rates and levels of perfusion (contrast intensity change over time) are plotted for representative animals.

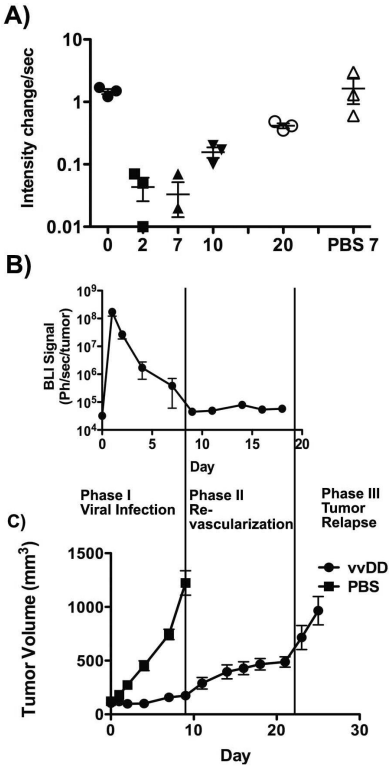

Figure 2.

Kinetics and levels of vascular collapse and re-perfusion. **(A)** Quantification of changes in tumor perfusion at different times after viral treatment are shown (n=3; experiment repeated three times)(perfusion change between day 0 and 2, p=0.0006). **(B)** Viral gene expression levels. Viral luciferase transgene expression from within the tumor was also determined by whole animal bioluminescence imaging at the indicated times subsequent to IP luciferin substrate injection (n=8). **(C)** Tumor growth was determined by caliper measurement for the same animals, along with PBS treated controls (n=8).

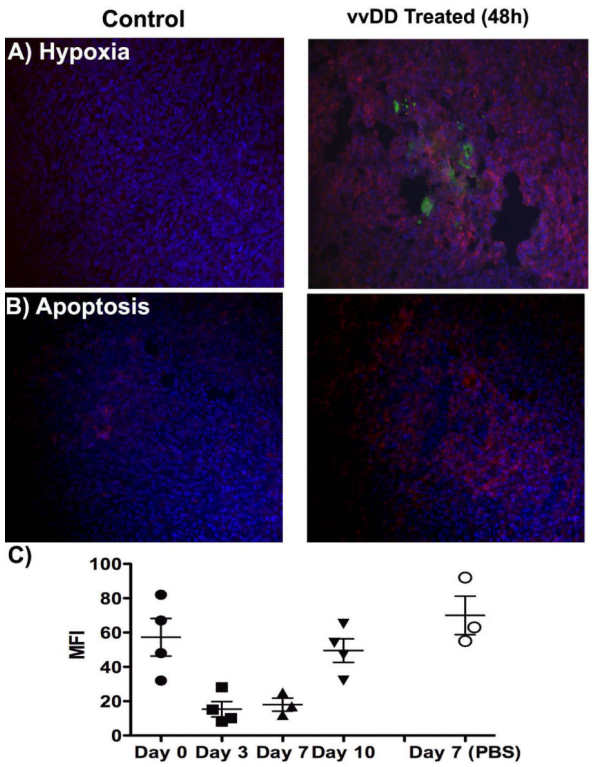

Figure 3.

Viral-mediated tumor vascular collapse leads to profound anti-angiogenic changes within the tumor microenvironment. **(A)** Hypoxic regions in the tumor. Mice (BALB/c mice with 4T1 subcutaneous tumors treated intravenously with 1×10^8 PFU of vvDD 48h earlier) were injected intravenously with Hypoxyprobe 15 minutes prior to sacrifice. Hypoxic regions were then stained post mortem (red) along with virus (green) and nuclei (Hoescht; blue); **(B)** Apoptosis within the tumor. Apoptosis was also determined with annexin-V staining (red) on sections post mortem 48h after treatment **(C)** VEGF levels in the tumor. In an additional experiment mice were sacrificed at the indicated times after vvDD (or PBS) treatment as before. Levels of VEGF within the tumor were determined by Luminex assay (MFI= Mean Fluorescence Intensity; VEGF levels between day 0 and 3; p=0.012).

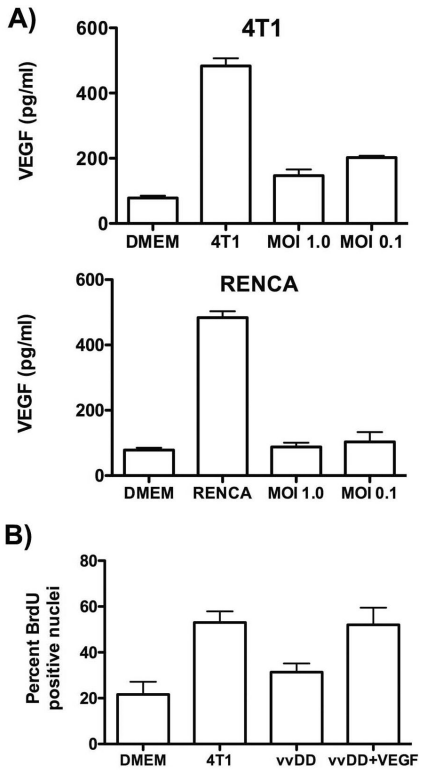

Figure 4.

Anti-angiogenic effects of oncolytic vaccinia therapy *in vitro*; **(A)** Production of VEGF as determined by ELISA in DMEM media alone and from conditioned medium collected from 4T1 or Renca cells alone or 24h after infection (MOI of 1.0 or 0.1) with vvDD; **(B)** Effects of conditioned medium from uninfected 4T1 cells or infected 4T1 cells (MOI 1.0 and 0.1, and filter sterilized at 0.1 μm to remove any viral particles) on proliferation of HUVEC, as determined by BrdU assay.

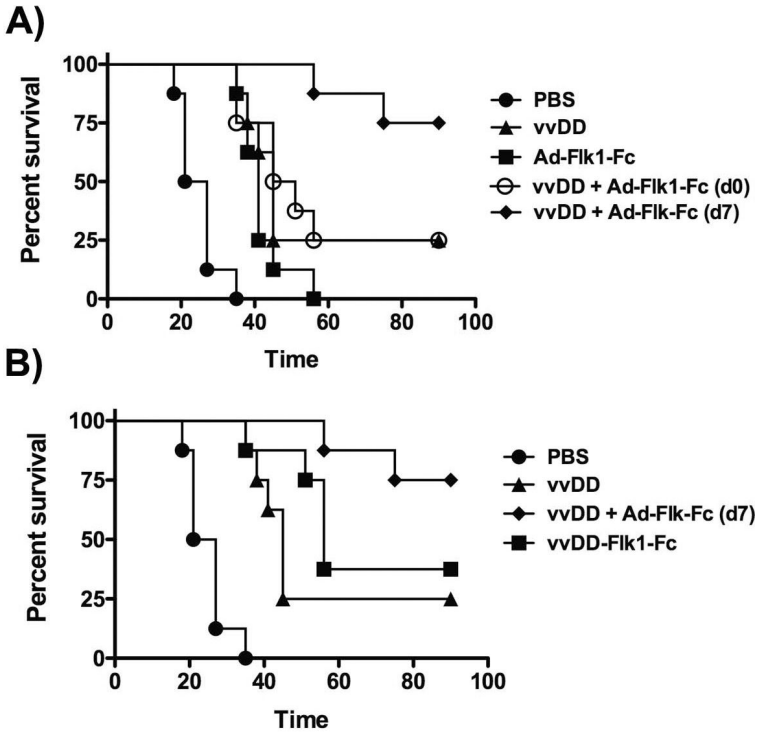

Figure 5.

Combination of oncolytic vaccinia with anti-angiogenic gene therapy. **(A)** Importance of timing of therapy combinations. Mice (athymic nu-/nu- with subcutaneous MDA-MB-231 tumors were treated intravenously with 1×10^8 PFU of vvDD or 1×10^{10} PFU of Ad-Flk1-Fc (non-replicating Ad expressing Flk1-Fc); or combinations of both with the Ad-Flk1-Fc delivered either on the same day as the vvDD (day 0) or 7 days after vvDD treatment. Subsequent tumor growth was followed with mice reaching the endpoint for sacrifice when tumors reached $1400mm^3$. (n=8 per group)(vvDD + Ad Flk1-Fc applied on day 0 verses day 7, p=0.019). **(B)** Combination vvDD and Flk1-Fc gene therapy produces enhanced therapeutic benefit relative to vvDD expressing Flk1-Fc. In a repeat experiment an additional group expressed the Flk1-Fc directly from the virus. (vvDD + Ad Flk1-Fc (d7) verses vvDD-Flk1-Fc, p=0.032)

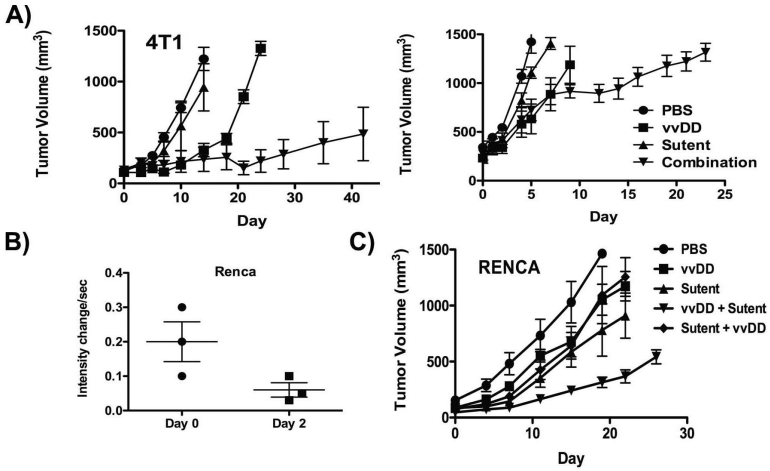

Figure 6.

vvDD combination therapy with suntininb (Sutent). **(A)** Mice (BALB/c) bearing 4T1 (either small tumors (50-100mm^3; left panel) or large tumors (300-400mm^3; right panel)) were treated with 1×10^8 PFU vvDD or sunitinib, or the combination of both, with sunitinib therapy beginning 7 days after vvDD treatment. Subsequent tumor growth was followed by caliper measurements (n=8 per group)(combination group performs statistical better than all other treatment groups ($p<0.05$) from day 21 (4T1 small); or day 12 (4T1 large); **(B)** Vascular collapse in Renca tumor model. Mice (BALB/c bearing subcutaneous Renca tumors and treated intravenously with 1×10^8 PFU of vvDD) were imaged for tumor perfusion levels by contrast enhanced ultrasound before and 48h after viral treatment ($p=0.08$). **(C)** Anti-tumor effects of vvDD used in combination with sunitinib in Renca tumors. Mice (BALB/c) bearing Renca tumors (50-100mm^3) were treated with 1×10^8 PFU vvDD or sunitinib, or the combination of both, with sunitinib therapy beginning 7 days after vvDD treatment or 7 days before vvDD treatment. Subsequent tumor growth was followed by caliper measurements (n=8 per group)(combination group (vvDD then sunitinib) performs statistical better than all other treatment groups ($p<0.05$) from day 15).